THE ASTROPHYSICAL JOURNAL, 355:L51–L54, 1990 June 1

CO AND *IRAS* DETECTION OF AN INTERMEDIATE-VELOCITY CLOUD

F.-X. DÉSERT
DEMIRM, Observatoire de Meudon
D. BAZELL
Space Telescope Science Institute
AND
L. BLITZ
Astronomy Program, University of Maryland
Received 1989 December 11; accepted 1990 March 20

ABSTRACT

In the course of a radio CO survey of high Galactic latitude clouds, we detected CO emission at the position $l = 210.^{\circ}8$ and $b = 63.^{\circ}1$ with an LSR velocity of -39 km s^{-1}. This molecular cloud constitutes the third one with an unusually large absolute velocity at these latitudes, as compared with the 5.4 km s^{-1} cloud-to-cloud velocity dispersion of the high-latitude molecular clouds. The position is coincident with an H I intermediate-velocity cloud: (GHL 11, Verschuur H, OLM 268), and an infrared-excess cloud 306 in the list by Désert, Bazell, and Boulanger (i.e., it shows more infrared emission than can be accounted for by the H I gas alone). This cloud is clearly detected at all four *IRAS* wavelengths and has warmer colors than the local interstellar medium. It shows evidence for grain processing because of spatial variations of the IR colors. It may be part of the supernova remnant that has been hypothesized to explain some high-latitude IVCs or may belong to family of comet-like clouds found by Odenwald. We therefore propose the existence of a new population of molecular clouds, the ones at intermediate H I velocities and high latitudes, which to date contains three known members.

Subject headings: infrared: general — interstellar: grains — interstellar: molecules

I. INTRODUCTION

The H I surveys of the high Galactic sky long ago revealed the existence of a gaseous component at unexpected velocities (Blaauw and Tolbert 1966; Hulsbosch and Raimond 1966). This component has been more or less arbitrarily subdivided into the intermediate-velocity clouds (IVCs: $20 \leq |v| \leq 90$ km s^{-1}) and the high-velocity clouds ($|v| \geq 90$ km s^{-1}), following the subdivision by Meng and Kraus (1970). The origin of the high-velocity H I gas is still a matter of controversy, but the two possible interpretations for the IVCs are (1) that a supernova close to the Sun ejected some material less than a million years ago (Oort 1966; Verschuur 1971) or (2) an external H I gas complex is falling into the Galaxy (Wesselius and Fejes 1973).

Désert, Bazell, and Boulanger (1988, hereafter DBB), have given a catalog of high-latitude ($|b| \geq 5^{\circ}$) infrared excess clouds (IRECs) i.e., clouds that have significantly more 100 μm (*IRAS*) emission than can be accounted for by the H I medium only (at velocities between -92 and 75 km s^{-1}). We have conducted a CO survey, described elsewhere (Bazell, Blitz, and Désert 1990), of these IRECs. They are apparently primarily diffuse high-latitude molecular clouds with a low CO abundance which is characteristic of CO–poor molecular clouds (Lada and Blitz 1988; Blitz, Bazell, and Désert 1990), although some IRECs are also produced by local heating sources. Two detections of CO were made that correspond to intermediate-velocity atomic hydrogen clouds. One of them is the well-known Draco Nebula studied by Mebold *et al.* (1985: G90.0+38.6−25), and Magnani, Blitz, and Mundy (1985, hereafter MBM: clouds 41–44). In this *Letter*, we report the intermediate-velocity CO detection of cloud 306 in the list of IRECs by DBB (G210.8+63.1−38.7). Reach, Heiles, and Koo (1989) have independently observed CO in this latter cloud and another new molecular IVC (G135.3+54.5−45; Heiles, Reach, and Koo 1988 and W. T. Reach, private communication). In § II, we detail the radio observations, and in § III, we analyze the *IRAS* maps of the 2° by 2° region surrounding the IVC. Finally, in § IV, we discuss the possible nature of this cloud and its origin, through the analysis of its spatial structure revealed by *IRAS*.

II. CO OBSERVATIONS

The radio observations were first carried out using the National Radio Astronomy Observatory 12 m telescope at Kitt Peak on 1988 March 4–7. The CO ($J = 1 \rightarrow 0$, $\nu = 115.2712$ GHz, HPBW $\simeq 60''$) transition was observed with a helium-cooled SIS receiver giving a typical system temperature of less than 600 K at the zenith. An arbitrary reference position was obtained by switching 1° (west) in azimuth. Only one position was observed in the area of the IVC due to time constraints. It was the local maximum of the 100 μm brightness in a 2° by 2° map centered on the position given by DBB (cloud 306) and extracted from *IRAS* skyflux plate 58 (HCON 1; see the Explanatory Supplement 1988). The 1950 coordinates of the infrared maximum position are $\alpha = 10^{h}49^{m}0^{s}$, $\delta = 25^{\circ}13'07''$ ($l = 210.^{\circ}8$, $b = 63.^{\circ}1$). Six integrations of 5 minutes each were obtained. The first was obtained on March 4, and the following five were obtained on March 7. All six spectra were averaged in order to improve the signal-to-noise ratio. Figure 1*a* is the observed spectrum which shows a line at a velocity of -38.7 km s^{-1} at the peak corresponding to $T_A^* = 0.41 \pm 0.05$ K at a resolution of 0.65 km s^{-1}. No signal was detected at velocities (with respect to the local standard of rest) between -33 and 33 km s^{-1} at a 1 σ level of 0.15 K and a

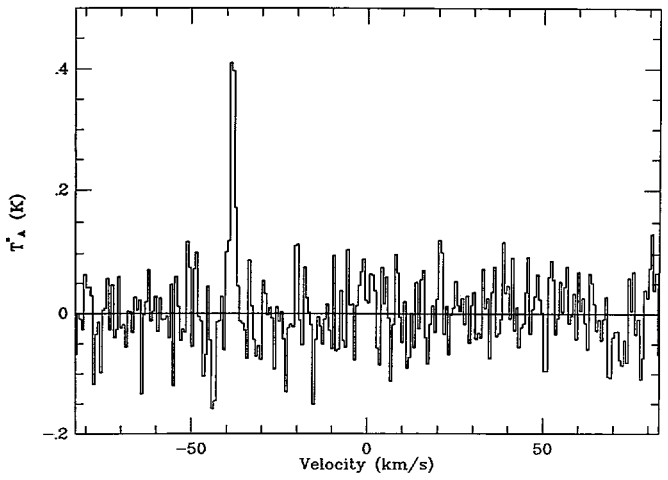

FIG. 1*a*

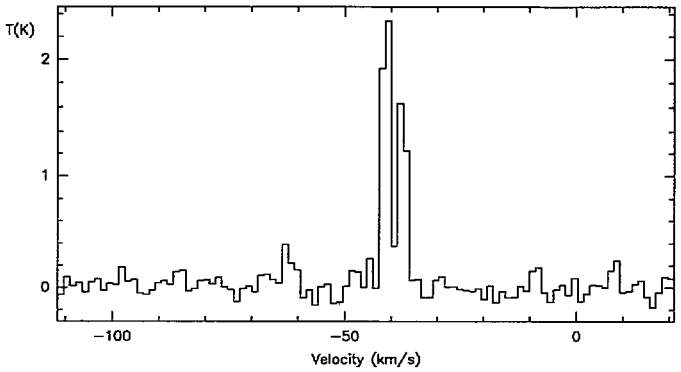

FIG. 1*b*

FIG. 1.—Two CO spectra of the intermediate-velocity cloud (G210.8+63.1−39) are shown. (*a*) Kitt Peak 30 minute spectrum at the frequency of the CO (1–0) rotational transition on the center clump. The antenna temperature of the signal is shown as a function of the velocity with respect to the local standard of rest. (*b*) IRAM 4 minute spectrum at the frequency of the CO (2–1) rotational transition on the eastern clump. The radiation temperature is shown as a function of the heliocentric velocity ($=v_{LSR}+0.43$ km s^{-1}).

resolution of 0.33 km s^{-1}. The CO line integrated intensity is $I_{CO}=0.77\pm0.06$ K km s^{-1}, with a FWHM of 1.9 km s^{-1}. *A posteriori*, we found an associated H I feature at the same velocity as the CO line in the velocity-position H I map of Heiles and Habing (1974). On the other hand, there is very little H I emission at low velocities above the 2 K emission level. This well-defined IVC has been detected in the H I 21 cm transition by Meng and Kraus (1970) as cloud OLM 268 (211.08+63.12), Verschuur (1971) as cloud H (208.6+61.5), and Wesselius and Fejes (1973) as part of the cloud GHL 11 (210+62.5).

An additional radio observation was made on 1989 January 6 with the IRAM 30 m telescope in Pico Veleta near Grenada (Spain). The CO ($J=2\rightarrow1$) second transition, at $\nu=230.538$ GHz, with a small-beam HPBW$\simeq14''$ was observed with a helium-cooled SIS receiver giving a typical system temperature of 930 K. Anticipating the infrared maps introduced in next section, the observed position ($\alpha=10^h50^m21^s.2$, $\delta=25°12'07''$) corresponds to the eastern clump of the IVC, with a reference position carefully chosen outside the IVC ($\alpha_r=10^h52^m00^s.0$, $\delta_r=25°00'00''$), the pointing accuracy being 3″. Figure 1*b* shows the spectrum obtained with a 4 minute integration on a filterbank of 512 channels of 1 MHz giving a velocity resolution of 1.3 km s^{-1}. The striking feature of this spectrum is the double-peaked line at the IVC velocity. Other positions were observed within two beams of the given position showing that the strength of the two peaks is highly variable.

Unfortunately, no high-spatial and high-spectral resolution H I map exists at present. Hence, we can turn to the dust emission as a gas tracer at high resolution (e.g., Boulanger, Baud, and van Albada 1984; Weiland *et al.* 1986) under the assumption of a constant gas-to-dust ratio.

III. *IRAS* OBSERVATIONS

The IVC is clearly detected in the infrared, and the morphology and velocity structure of the cloud suggest that it has been subjected to a shock. Therefore we can hope to study in this cloud how dust is processed by shocks. Moreover, because little gas (H I or CO) is detected at other velocities, we can assume that, other than the foreground zodiacal emission, all of the infrared emission corresponds to the IVC. The *Infrared Astronomical Satellite* (*IRAS*) data at the four bands centered on 12, 25, 60, and 100 μm have been analyzed in a field of 2° by 2° centered on the DBB position. The field was observed 3 times during the course of the *IRAS* mission, and we used the co-added data on this field provided by the Infrared Processing and Analysis Center (IPAC). These data show major improvements compared with individual sky-flux plate subimages (*IRAS Explanatory Supplement* 1988) in calibration, spatial resolution, signal-to-noise ratios, and destriping. Therefore, they have been used hereafter. The improvements due to co-adding data are critical if we consider the faintness of the IVC under consideration. The spatial resolution varies with different *IRAS* bands. Hence, the data were smoothed to an identical resolution of 3′ × 5′ (the 100 μm resolution) with a pixel size of 1 arcminute^2. Each detector baseline was adjusted before projection onto the final map so that no stripes are apparent.

Zodiacal emission dominates the two short-wavelength bands and is present to a lesser extent in the two others. Hence, this foreground emission needs to be removed from the maps before analysis of the interstellar dust emission. Zodiacal emission is assumed to be smooth throughout the map. It was computed by fitting a second-order two-dimensional polynomial to the brightness of pixels outside obvious clumpy emission (as defined by the 100 μm map and point sources). The four foreground-subtracted maps are shown in Figure 2 (Plates L1–L4).

The 12, 60, and 100 μm maps are quite similar in morphology. We note two large clumps of matter, one at the center, and the other on the eastern side which are both detected in CO (see previous section). The map is also very asymmetric in the sense that there is a smooth decrease of emission toward the west part as compared with the sharp emission gradient of the eastern clump. The similarity of the maps at different wavelengths is emphasized by doing a correlation plot. Figure 3 shows the correspondence between the brightnesses at 60 and 100 μm for each pixel of the sky (resolutions have been made identical for that reason). The 60 to 100 μm slope has a bimodal distribution with a main part centered at a ratio of

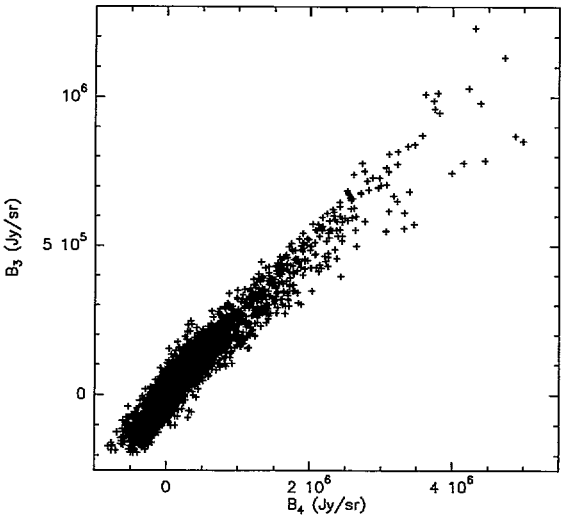

FIG. 3.—Pixel-to-pixel correspondence between background-subtracted maps of the IVC at 60 and 100 μm. For clarity, only one-quarter of the pixels have been plotted. There is no offset in the correlation between the brightness at 60 μm (B_3) and 100 μm (B_4). One notes a bimodal distribution of the ratio B_3/B_4, being either 0.26 for the larger number of pixels and 0.18 for a smaller number of pixels which are all located in the eastern clump of the cloud (see Fig. 2*d*).

$B_\nu(60)/B_\nu(100) = 0.26$ and a secondary part at 0.18. In a map of the ratio, the lower ratio corresponds exactly to the eastern clump. The 25 μm map, although more noisy, still shows the cloud as delineated by the 100 μm map, except for the northern part of the IVC which is absent at 25 μm.

IV. DISCUSSION

a) Infrared Properties

We can undoubtedly associate the main cloud, observed in the four infrared maps, with the IVC observed in H I and CO data, showing that IVCs contain heavy elements and dust (see Odenwald and Rickard 1987 for the Draco nebula); hence, they cannot be made of primordial extragalactic material. On the contrary, Wakker and Boulanger (1987) have shown that *high-velocity* ($|v| \geq 90$ km s^{-1}) clouds do not emit in the infrared and therefore are either devoid of dust or the dust-to-gas ratio is at most a factor of 0.5–0.25 its normal value. However, the infrared colors of the IVC are not the same as those of the interstellar dust in the solar neighborhood. The 60 to 100 μm brightness ratio in the main part of the clump (0.26) is larger than the ratio (0.21 ± 0.02) obtained from the cosecant law by Boulanger and Pérault (1988, hereafter BP) or the ratio (0.17 ± 0.01) of typical molecular high-latitude clouds (Weiland *et al.* 1986). Heiles, Reach, and Koo (1988) have also found a larger ratio for IVCs (0.29 ± 0.02) than for normal velocity clouds (0.21 ± 0.01). Hence the color temperature (using a λ^{-2} emissivity law) is larger by about 1.5 K from the "standard" 22.5 K, which means that either (1) the dust heating is increased by $\sim 50\%$ from the usual interstellar radiation field or (2) very small grains that contribute to the 60 μm band are more abundant. In the first interpretation, this heating could be due to the shock encountered by the cloud which is being braked by the local diffuse medium. Moreover, the shock is strongly suggested by the infrared morphology of the cloud. However, in this interpretation, it is not clear why the eastern clump has a *lower* temperature (21.5 K) than the center clump whereas it seems to be more exposed to the shock heating. The alternative interpretation comes from the strong suggestion that, in the diffuse interstellar medium, the emission shortward of 80 μm can best be explained by the existence of very small grains which have temperature fluctuations under individual photon absorption (Draine and Anderson 1985, BP, and references therein). In this case, the 60 to 100 μm ratio provides a measure of the abundance of grains of size between 3 and 10 nm relative to the bigger grains that emit at their equilibrium temperature. The stronger shock on the eastern clump may have destroyed the small grains responsible for part of the 60 μm emission. Evidence for grain processing by shocks have been given by various authors using the extinction curve (e.g., Seab and Shull 1983) or the infrared properties (Heiles, Reach, and Koo 1988). At the shorter *IRAS* 12 and 25 μm bands, the IVC is clearly detected but has a more clumpy morphology that is probably due to a lower signal-to-noise ratio. From the ratio of 12 and 25 μm emission to the 100 μm emission, one can deduce that the cloud is not special at these wavelengths compared with the local interstellar medium. Hence the IVC is likely to contain small grains of radius between 0.5 and 5 nm and/or large molecules like polycyclic aromatic hydrocarbons (PAHs) (see, e.g., Puget and Léger 1989). However, the clumping at 12 and 25 μm could also indicate that the abundance of very small particles is not constant in the IVC.

If we spatially define the cloud by the contour level of 1 MJy sr^{-1} at 100 μm, then we can integrate the brightness inside the cloud to find the total flux that it emits. We find that at 12, 25, 60, and 100 μm, the cloud fluxes are, respectively, 7.4 ± 0.2, 7.4 ± 0.3, 53.4 ± 0.3, 227 ± 1 Jy within an area of 0.41 deg^2, the error bars being computed from the rms brightness of pixels outside the cloud. Note that the global 60 to 100 μm flux ratio (0.24) is in agreement with the two values (0.26 and 0.18) given above.

The emission by two stars can be seen in the near-infrared *IRAS* maps shown in Figure 2. These are the double A stars SAO 81583 and 81584 (10529+2500) and the 10th mag red variable RU Leo (10504+2441, also variable in *IRAS* data) whose infrared emission can be seen in the four *IRAS* bands. It is not clear whether the stars are associated to the IVC or not.

b) Visible Properties

Inspection of the Palomar plate including this region did not reveal any nebulosity at the position of the IVC. However, its faintness in the infrared (related to the scattering in the visible) might explain that observation. A blue object known as TON 44 ($m_{pg} = 15.9$; Iriarte and Chavira 1957) lies in the middle of the cloud (10:50.0+25:16). M. Dennefeld (private communication) has kindly taken a visible spectrum of this object at the Observatoire de Haute-Provence revealing that it is a white dwarf. Indeed, if it were at a distance of 100 pc, it would have the optical luminosity ($M \simeq +11$) and the color (much bluer than A0) of a young white dwarf. One does not know if it is associated with the IVC, but this object could be used as a probe of the absorption properties of the IVC if it lies behind the cloud.

c) Radio Properties

The H I observations suggest that the IVC is part of a bigger cloud complex which has a spatial extent of at least $1° \times 3°$ (Verschuur 1971) and $3° \times 8°$ (Meng and Kraus 1970) and a velocity extent of about ± 4 km s^{-1} (i.e., wider than the CO width of ± 1 km s^{-1}). From the integrated CO line I_{CO}

observed in the center clump, one can infer an H_2 column density of about $1.9 \pm 0.2 \times 10^{20}$ cm^{-2}, assuming a conversion ratio of $N(H_2)/I_{CO} = 2.5 \times 10^{20}$ cm^{-2}/(K km s^{-1}) (Bloemen *et al.* 1986). For the eastern clump, the estimated column density is 10 times stronger (2.4×10^{21} cm^{-2}). These column densities can be compared with the H I column density given by Verschuur (1971) of 0.9×10^{20} H cm^{-2} (although in a larger beam of 10′), which may suggest that the molecular gas has condensed from the atomic gas.

d) Physical Properties

One can estimate the mass of the IVC by using its infrared emission and assuming that the dust-to-gas ratio is normal in this cloud. According to BP, the ratio of the infrared emission at 100 μm to the hydrogen column density is of the order of 1 MJy sr^{-1} (10^{20} H cm^{-2})$^{-1}$ which, with the integrated flux of the cloud of 227 Jy at 100 μm, yields an estimate of 1.8 $M_\odot$ at a distance of 100 pc. This estimate can be compared with the H I mass of the IVC complex of 8.7 $M_\odot$ (Verschuur 1971) deduced for a larger area. The assumed distance of 100 pc is consistent with the estimate by Wesselius and Fejes (1973) from calcium visible absorption line for the distance of a nearby IVC NHX 210+70−42 (between 12 and 400 pc). At this distance the cloud has a linear size of 1.2 pc.

e) A New Class of Molecular Clouds?

To date, two other clouds detected have been reported that share the following properties of the IVC shown here: (1) they are detected in H I, in the infrared (*IRAS*), and in CO radio lines, and (2) they are at high Galactic latitudes ($|b| \geq 20°$); and (3) they have unusual velocities ($|v| \geq 20$ km s^{-1}) compared with the local high-latitude molecular clouds which show a zero average velocity (with respect to LSR) with a cloud-to-cloud velocity dispersion of only 5.4 km s^{-1} (MBM). These are (1) the Draco nebula (Mebold *et al.* 1985 and MBM) and (2) cloud G135+54−45 (Heiles, Reach, and Koo 1988). Therefore, we are probably encountering a new class of faint clouds satisfying the above properties that we call intermediate-velocity molecular clouds (IVMCs). We note that the three known IVMCs all have negative velocities which may point to a common origin. These clouds probably belong to the more general class of comet-like clouds studied by Odenwald (1988) which owe their appearance to shocks with the ambient diffuse medium. The IVC studied here is part of a larger ring structure which is barely visible in *IRAS* skyflux plate centered on ($\alpha = 10^h45^m$, $\delta = +26°$) and with a diameter of $\sim$4°. More radio and infrared observations are clearly needed, especially to elucidate the kinematic structure of this cloud.

f) Summary

We have analyzed a 0.5 deg^2 cloud made of atomic and mostly molecular gas, and dust. It is located at a very high Galactic latitude (63°) and with an unusual velocity (−39 km s^{-1}) toward the Galactic plane. Its interaction with the diffuse interstellar medium is shown as plumed trailing on the back side of the main two clumps, as some possible grain processing (destruction of a certain class of small grains) shown as a colder 60 to 100 μm color in the eastern clump, and complex CO line profiles. At a likely distance of $\sim$100 pc, the lifetime of this cloud, as well as other IVMCs, is at most a few million years (Odenwald 1988).

We thank D. T. Leisawitz for kindly providing a background subtraction program as well as for helpful suggestions, IPAC for having quickly produced the co-added data, and F. Boulanger for discussions. We thank M. Dennefeld for kindly making additional observations for us and F. Viallefond for helping in the IRAM observations and reductions. This work was done while one of us (F.-X. D.) held a National Research Council research associateship at the Infrared Astrophysics Branch, Laboratory for Astronomy and Solar Physics, NASA/Goddard Space Flight Center. L. B. gratefully acknowledges support from NSF grant 86-18763 and JPL 958009.

REFERENCES

Bazell, D., Blitz, L., and Désert, F.-X. 1990, in preparation.
Blitz, L., Bazell, D., and Désert, F.-X. 1990, *Ap. J. (Letters)*, **352**, L13.
Blaauw, A., and Tolbert, C. R. 1966, *Bull. Astr. Inst. Netherlands*, **18**, 405.
Bloemen, J. B. G. M., *et al.* 1986, *Astr. Ap.*, **154**, 25.
Boulanger, F., Baud, B., and van Albada, G. D. 1985, *Astr. Ap.*, **144**, L9.
Boulanger, F., and Pérault, M. 1988, *Ap. J.*, **330**, 964 (BP).
Désert, F.-X., Bazell, D., and Boulanger, F. 1988, *Ap. J.*, **334**, 815 (DBB).
Draine, B. T., and Anderson, N. 1985, *Ap. J.*, **292**, 494.
Heiles, C., and Habing, H. J. 1974, *Astr. Ap. Suppl.*, **14**, 1.
Heiles, C., Reach, W. T., and Koo, B. C. 1988, *Ap. J.*, **332**, 313.
Hulsbosch, A. N. M., and Raimond, E. 1966, *Bull. Astr. Inst. Netherlands*, **18**, 413.
IRAS Explanatory Supplement. 1988, ed. C. A. Beichman, H. J. Neugebauer, H. J. Habing, P. E. Clegg, and T. J. Chester (Washington, DC: GPO).
Iriarte, B., and Chavira, E. 1957, *Bol. Obs. Tonantzintla, y Tacubaya*, Vol. **2**, No. 16, p. 3.
Lada, E. A., and Blitz, L. 1988, *Ap. J. (Letters)*, **326**, L69.
Magnani, L., Blitz, L., and Mundy, L. 1985, *Ap. J.*, **295**, 402 (MBM).
Mebold, U., Cernicharo, J., Velden, L., Reif, K., Crezelius, C. and Goerigk, W. 1985, *Astr. Ap.*, **151**, 427.
Meng, S. Y., and Kraus, J. D. 1970, *A.J.*, **75**, 535.
Odenwald, S. F. 1988, *Ap. J.*, **325**, 320.
Odenwald, S. F., and Rickard, L. J. 1987, *Ap. J.*, **318**, 702.
Oort, J. H. 1966, *Bull. Astr. Inst. Netherlands*, **18**, 421.
Puget, J. L., and Léger, A. 1989, *Ann. Rev. Astr. Ap.*, **27**, 161.
Reach, W. T., Heiles, C., and Koo, B. C. 1989, in *IAU Symposium* 135, *Interstellar Dust*, ed. L. J. Allamandola and A. G. G. M. Tielens (Dordrecht: Kluwer), p. 499.
Seab, C. G., and Shull, J. M. 1983, *Ap. J.*, **275**, 652.
Verschuur, G. L. 1971, *A.J.*, **76**, 317.
Wakker, B. P., and Boulanger, F. 1986, *Astr. Ap.*, **170**, 84.
Weiland, J. L., Blitz, L., Dwek, E., Hauser, M. G., Magnani, L., and Rickard, L. J. 1986, *Ap. J. (Letters)*, **306**, L101.
Wesselius, P. R., and Fejes, I. 1973, *Astr. Ap.*, **24**, 15.

D. Bazell: Space Telescope Science Institute, 3700 San Martin Drive, Baltimore, MD 21218

L. Blitz: Astronomy Program, University of Maryland, College Park, MD 20742

F.-X. Désert: DEMIRM, Observatoire de Meudon, 92195 Meudon Cedex, France

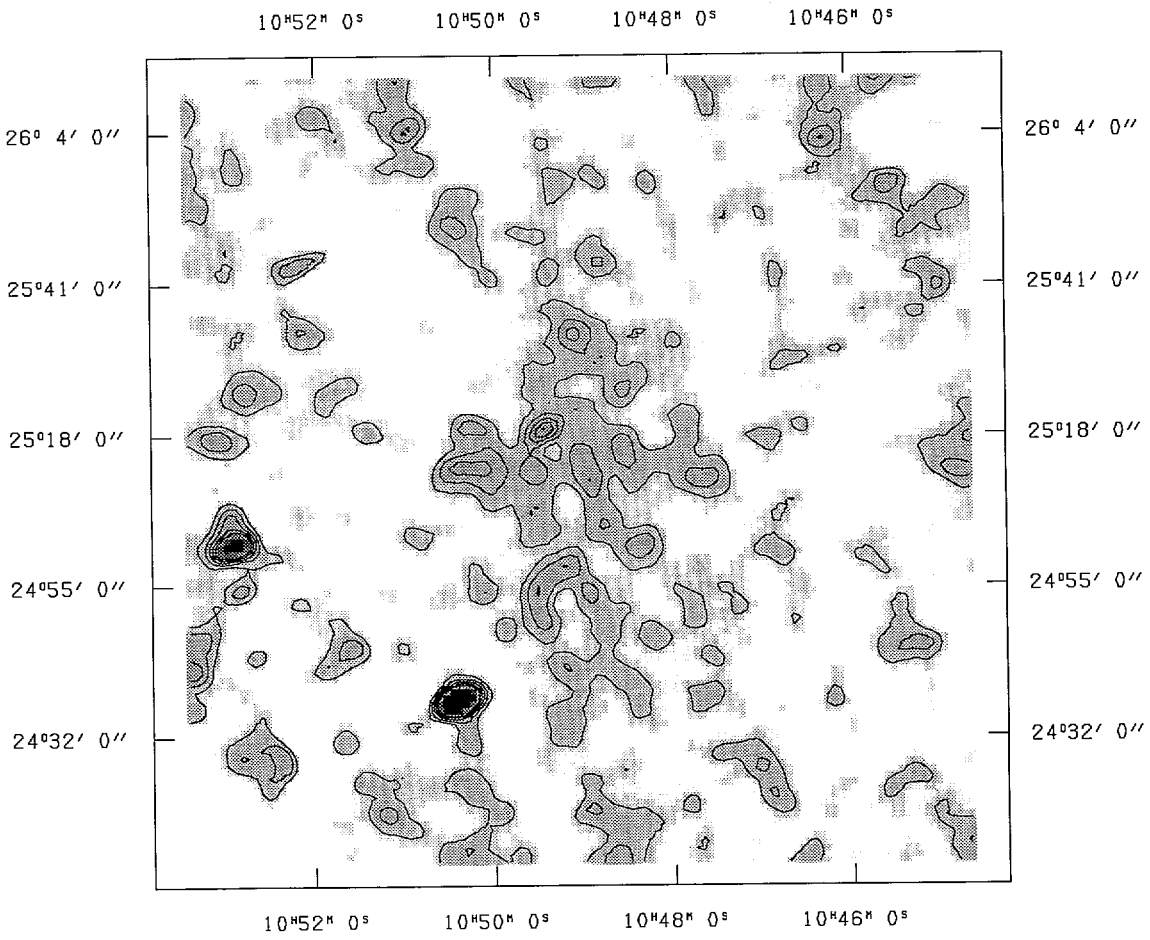

FIG. 2a

FIG. 2.—Infrared maps of a 2° × 2° field centered on the IVC at (*a*) 12 μm, (*b*) 25 μm, (*c*) 60 μm, and (*d*) 100 μm. These maps are co-added *IRAS* data from which a smooth background has been subtracted (see text). The resolution was diminished to 3′ × 5′ for all maps (the resolution at 100 μm). Some point sources (especially at 12 μm) give the equivalent beam size. One notes the extreme similarity of the 60 and 100 μm maps as well as sharp gradients particularly on the east side. An orthographic projection has been used here, and output brightnesses are in Jy sr^{-1} at the center wavelength of each band, assuming a constant νB_ν emission law in the *IRAS* band filter. Contours are by increments of, respectively, 5×10^4, 7.5×10^4, 7.5×10^4, and 2.5×10^5 Jy sr^{-1} and start at the increment unit level. The gray scale follows the contours.

PLATE L2

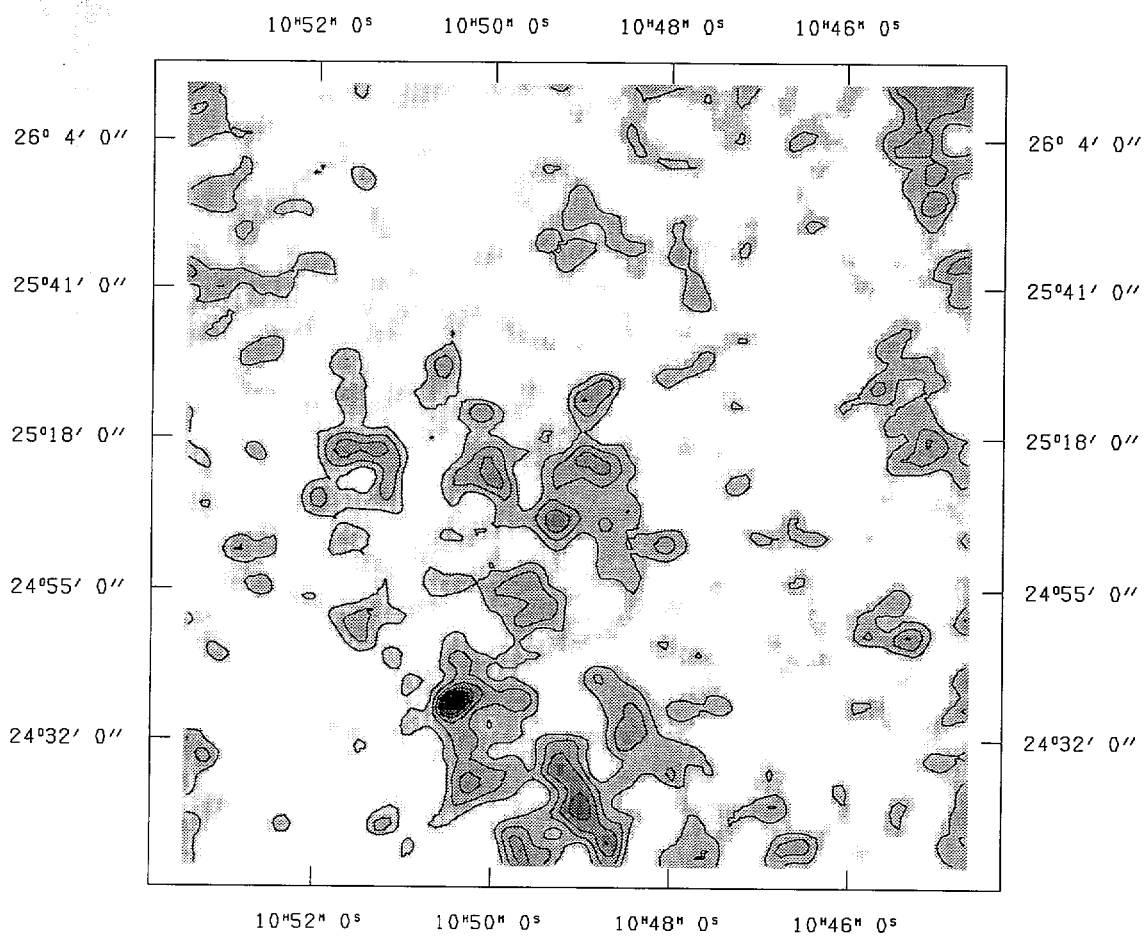

FIG. 2*b*

DÉSERT, BAZELL, AND BLITZ (*see* **355**, L52)

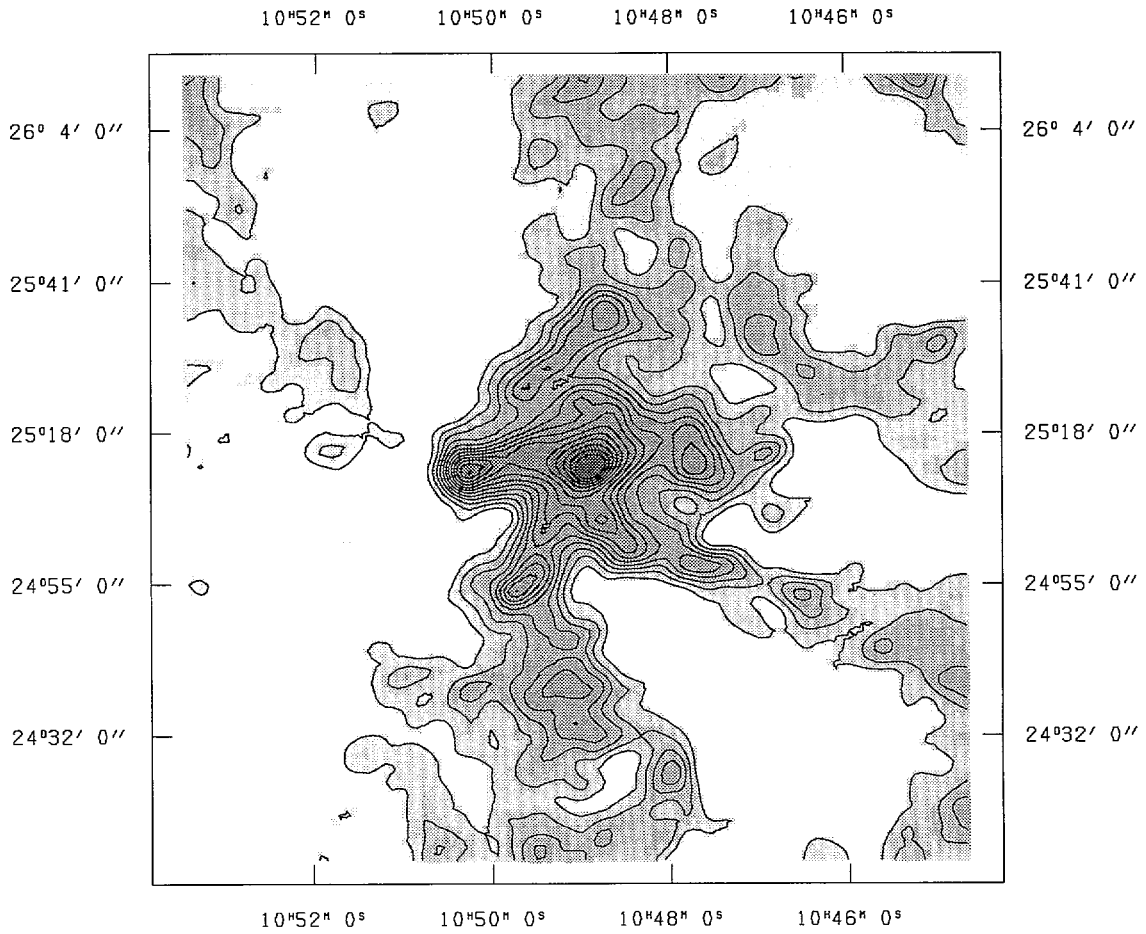

FIG. 2*c*

DÉSERT, BAZELL, AND BLITZ (*see* **355**, L52)

PLATE L4

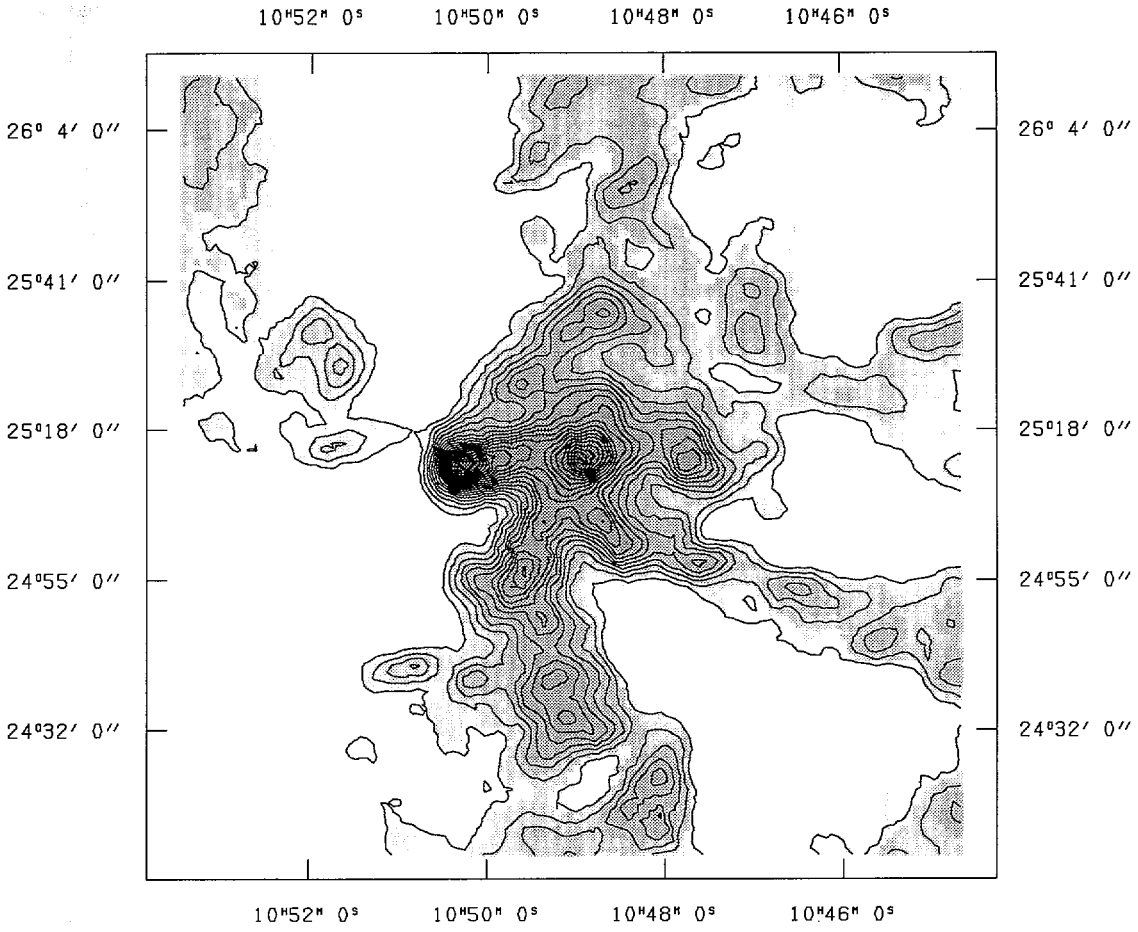

FIG. 2*d*

DÉSERT, BAZELL, AND BLITZ (*see* **355**, L52)